International Journal of Mass Spectrometry 333 (2013) 8–14

Contents lists available at SciVerse ScienceDirect

International Journal of Mass Spectrometry

journal homepage: www.elsevier.com/locate/ijms

Advantages of pyrene derivatization to site-specific glycosylation analysis on MALDI mass spectrometry

Takashi Nishikaze, Hisako Okumura, Hiroshi Jinmei, Junko Amano*

Laboratory of Glycobiology, The Noguchi Institute, 1-8-1 Kaga, Itabashi, Tokyo 173-0003, Japan

ARTICLE INFO

Article history:
Received 17 February 2012
Received in revised form 2 August 2012
Accepted 2 August 2012
Available online 10 August 2012

Keywords:
Glycopeptide
Glycoform
MALDI
DHBA
Signal localization

ABSTRACT

Glycoproteomics involving the analysis of glycopeptides by matrix-assisted laser desorption/ionization mass spectrometry (MALDI-MS) is a new and attractive technique. However, quantitative performance in MALDI-MS is hampered by its poor reproducibility among laser shots. 2,5-Dihydroxybenzoic acid (DHBA) is a useful matrix for glycopeptides but forms highly heterogeneous crystals. In this study, we have investigated the distribution of significant signals generated from a sample of glycopeptides on the target plate using a MALDI imaging technique. MALDI images of glycopeptides, which have different glycans on the same peptide, in the Lys-C digests of bovine ribonuclease B were identical. Thus, all glycoforms on a given peptide can be detected at the same laser irradiation spot simultaneously, which offers a significant advantage over other techniques. A similar result was observed with glycopeptides of human serum immunoglobulin G. Interestingly, distinct MALDI images were observed for glycopeptides having different amino acid sequences, despite having an identical glycan structure. The common peptides, which were glycosylated or non-glycosylated, or sialylated or desialylated gave similar MALDI images. Taken together, our results suggest that sweet spot localization of glycopeptides is dependent on the peptide moiety rather than the glycan structure. Furthermore, introduction of pyrene group to glycopeptides which have different peptides result in a uniform MALDI image. It suggested that pyrene derivatization in MALDI-MS facilitates straightforward analysis of a glycopeptide mixture because the same mass spectrum can be obtained at every sweet spot in addition to increase in signal intensity. Thus, this study validates the use of MALDI-MS for site-specific glycoprofiling at the glycopeptide level.

1. Introduction

In recent years, glycoproteomics has become an important field of post proteomics approaches. A glycoprotein exists as a mixture of different glycosylated species named glycoforms. To clear this microheterogeneity is indispensable to characterization of the glycoprotein because glycoforms vary biological activities. Furthermore, if a glycoprotein has multi glycosylation sites, site-specific glycoprofiling, which provides a quantitative map of glycans attached to a given protein glycosylation site, is an important approach to clearly defining the function of a glycoprotein. It is essential to analyze glycopeptides without releasing glycans to prevent from destruction of the protein moiety. It is the best that all the glycoforms can be measured at once to know quantitative contents of glycoforms.

Mass spectrometry (MS) combined with a soft ionization technique has proven to be a powerful analytical tool for the analysis of glycopeptides [1,2]. Both electrospray ionization mass spectrometry (ESI-MS) [3] and matrix-assisted laser desorption/ionization mass spectrometry (MALDI-MS) [4–7] have been used to ionize fragile glycopeptides. MALDI-MS offers several advantages over ESI-MS for the analysis of a small amount of sample. In particular, MALDI-MS facilitates (i) relatively simple spectral interpretation; (ii) rapid analysis and (iii) repeated measurements of the same sample. Thus, MALDI-MS has been widely used in a variety of applications for the analysis of glycans and glycopeptides [8–12].

Although MALDI-MS is a very sensitive and precise method, it is difficult for quantification because ionization efficiency of analytes depends on their specific physicochemical properties. The ionization reaction of a glycopeptide, including protonation and deprotonation, mostly occurs on the peptide moiety. Thus, the signal intensity of a glycopeptide largely is dependent on the nature of the peptide portion, but only weakly dependent on the nature of glycan. Therefore, the glycoprofiling of glycopeptides based on their signal intensities should be possible because glycans are attached onto the same peptide. In fact, compared with different methods from MS, good correlation between signal intensities of glycopeptides and the actual amount of corresponding glycoform has been reported [13–15]. However, poor shot-to-shot and

* Corresponding author. Tel.: +81 3 3961 3255; fax: +81 3 3964 5588.
E-mail address: amano@noguchi.or.jp (J. Amano).

1387-3806/$ – see front matter © 2012 Published by Elsevier B.V.
http://dx.doi.org/10.1016/j.ijms.2012.08.006

sample-to-sample reproducibility in MALDI-MS may cause a problem in such quantitative measurements.

The poor reproducibility is considered to be particularly prominent when the matrix crystallizes heterogeneously. Although 2,5-dihydroxy benzoic acid (DHBA) is one of the most widely used matrices for ionizing glycans and glycopeptides, the matrix gives highly heterogeneous crystals. Typically, the long needle-like crystals exist mostly at the periphery, whereas thin microcrystals are distributed in the central region under standard dried-droplet preparation method. The appearance and intensity of analyte signal is highly dependent on the spot of laser irradiation over the crystallized matrix. Hence, significant variation in signal intensity is often observed. We have to measure all area of the matrix crystal and the signals obtained by all laser shots should be summed. To overcome the signal heterogeneity, many approaches have been suggested, including the production of a microcrystalline matrix [16], the fast evaporation of matrix solvent [17] and the use of liquid matrices [18]. However, these approaches can often promote undesirable alkali-metal adduction to the analyte. Bouschen and Spengler have suggested that relatively slow co-crystallization with matrix is an efficient sample-cleaning step in dried-droplet preparation [19].

Here, we used a MALDI imaging technique to investigate the distribution of signal spots of glycopeptides within MALDI samples. Originally, the MALDI imaging technique was applied to thin-layer chromatographic separation procedures [20] and for studying biological samples such as tissues [21]. Recently, several researchers have used MALDI imaging or a secondary ion mass spectrometry (SIMS) based imaging technique to investigate signal distribution in a sample prepared using the dried-droplet technique [19,22–24]. The results of these studies using lipids and peptides as analytes suggest that analyte signal distribution in DHBA matrix is highly heterogeneous, caused by segregation of each analyte in its physicochemical property.

In this study, we found that the MALDI images of glycoforms on the same peptide are identical to each other. We also demonstrate that pyrene derivatization of glycopeptides improves homogeneity and reproducibility of shot-to-shot spectra.

2. Experimental

2.1. Materials

Human serum albumin and bovine pancreatic ribonuclease B (RNaseB) were purchased from Sigma–Aldrich (Steinheim, Germany). Human immunoglobulin G (IgG) was purchased from WAKO Pure Chemical, Inc. (Osaka, Japan). Trypsin Gold (Mass Spectrometry Grade) and Lysyl Endpeptidase (Lys-C, Mass Spectrometry Grade) were purchased from Promega (Madison, WI) and WAKO Pure Chemical, Inc., respectively. Chymotrypsin from bovine pancreas (Sequencing Grade) was purchased from Roche (Penzberg, Germany). Cellulose fibrous medium was purchased from Sigma–Aldrich. The highly purified MALDI matrix chemicals, DHBA was purchased from Shimadzu-Biotech (Kyoto, Japan). Acetonitrile (LC/MS grade) and trifluoroacetic acid (TFA, HPLC grade) were purchased from Kanto Chemical Co., Inc. (Tokyo, Japan). The water used in all experiments was purified by using a NANOpure DIAMOND Ultrapure Water System from Barnstead (Boston, MA). All reagents were used without further purification.

2.2. Digestion of glycoproteins and protein

Albumin, RNaseB or IgG was incubated in 10 mM ammonium bicarbonate containing 10 mM dithiothreitol at 55 °C for 45 min. After cooling, 5 μL of 135 mM iodoacetamide was added to the mixture, which was then kept in the dark for 45 min. After adding RapiGest SF (Waters, Milford, MA) to a final concentration of 0.1% in 50 mM ammonium bicarbonate, the mixture was heated at 100 °C for 5 min. After cooling, the mixture was incubated with 1 μg of trypsin or Lys-C at 37 °C overnight. For chymotrypsin digestion, IgG was incubated in 100 mM Tris–HCl (pH 8.0) containing 10 mM $CaCl_2$ and 10 mM dithiothreitol at 55 °C for 45 min. After cooling, the sample was carbamidomethylated and denatured using RapiGest SF as described above. The mixture was incubated with 2 μg of chymotrypsin at 25 °C overnight.

The tryptic digest of albumin was desalted using a PepClean™ C-18 Spin Column (Pierce, Rockford, IL), and the digests of RNaseB and IgG were subjected to enrichment by hydrophilic interaction using cellulose fibrous medium [12,25].

For desialylation, enriched glycopeptide fractions derived from IgG were heated in 0.8% TFA at 80 °C for 45 min, and then dried using a Speed Vac.

2.3. Preparation of glycopeptides NA2-IRNKS and A2-I*RNKS

Disialylglycopeptide A2-KVANKT, A2-IRNKS, NA2-IRNKS, IRN(GlcNAc)KS and IRNKS were prepared as described previously [12]. Stable isotope-labeled A2-I*RNKS was prepared using Fmoc-Ile*-OH instead of Fmoc-Ile-OH. Ile*, in which six ^{13}C and one ^{15}N were substituted, is 7.017 Da heavier than non-labeled Ile.

2.4. On-plate pyrene derivatization

Some samples were directly derivatized by 1-pyrenyl diazomethane (PDAM, Molecular Probes, Inc., Eugene, OR) on the target plate as described previously [12]. The plate was well rinsed with xylene to remove excess amount of PDAM.

2.5. Mass spectrometry and MALDI imaging

Samples for MALDI-MS were prepared using standard dried-droplet technique. Analyte solution was first deposited on a mirror-polished stainless steel MALDI target. DHBA was dissolved in 60% acetonitrile/H_2O to a concentration of 10 mg/mL and 0.6 μL was applied onto the samples with or without on-plate pyrene derivatization and then left to dry without active air flow. All the above procedures were done in a clean room, where the temperature (23°) and humidity (50%) are controlled. Before measuring MS, the samples on the target plate were observed using a confocal laser microscope with 50× objective, LEXT OLS3100 (Olympus, Tokyo, Japan). MALDI-TOF mass spectra were acquired using an AXIMA-QIT instrument consisting of a quadrupole ion trap and reflector time-of-flight analyzer (Shimadzu Biotech, Manchester, UK). A nitrogen laser (337 nm) was used to irradiate the sample for ionization. Spectra in positive- and negative-ion modes were obtained with higher laser fluence than the threshold fluence for $[M+H]^+$ or $[M-H]^-$ ion detection. The samples were scanned by successive 10 laser shots with a spot-to-spot center distance of 50 μm in each direction to obtain a MALDI image. The MS data was converted to comma-separated values (CSV) and was visualized as MALDI image using graphical software Graph-R.

3. Results and discussion

3.1. Heterogeneity of signals in a sample of peptide mixture using DHBA as a matrix

DHBA forms small and large needle-shaped crystals from the rim of the target spot toward the center and the crystals is non homogeneity as shown in Fig. 1. This MALDI sample contains tryptic digest of human serum albumin consisted of more than 10 different peptides. Mass spectra a, b and c in Fig. 1 were obtained from

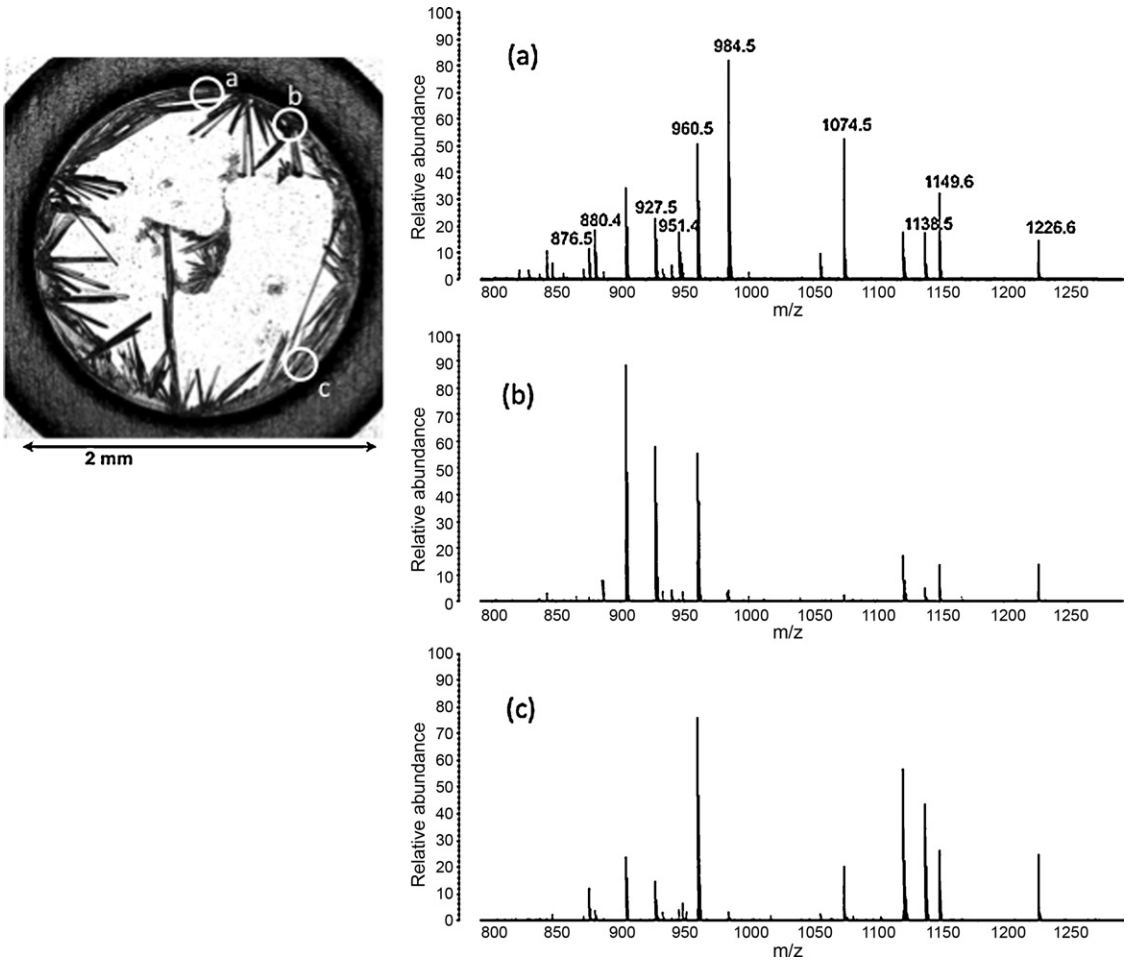

Fig. 1. Positive-ion mass spectra of peptides from a tryptic digest of human serum albumin at three positions (a)–(c) as highlighted in the confocal laser microscopy image of the MALDI sample. Identified peptides are as follows; the *m*/*z* ion 876.5, LCTVATLR; *m*/*z* 880.4, AEFAEVSK; *m*/*z* 927.5, YLYEIAR; *m*/*z* 951.4, DLGEENFK; *m*/*z* 960.5, FQNALLVR; *m*/*z* 984.5, TYETTLEK; *m*/*z* 1074.5, LDELRDEGK; *m*/*z* 1138.5, C (calbamidemethyl) C (calbamidemethyl) TESLVNR; *m*/*z* 1149.6, LVNEVTEFAK; *m*/*z* 1226.6, FKDLGEENFK.

three different locations (a, b and c in the same sample as shown in the microscopy image, respectively). The signal intensity patterns such as the ions at *m*/*z* 927.5, *m*/*z* 960.5 and *m*/*z* 1074.5 are significantly different among the three spectra. This result indicates that the signal intensity from each peptide varies depending on the precise position on the matrix of crystals. Such signal heterogeneity in a MALDI sample may cause serious problems in terms of quantification using MALDI-MS.

3.2. Common signal distribution of glycopeptides from RNaseB

We used glycopeptides of RNaseB to investigate whether signal distribution varies among glycopeptides. RNaseB is a well-characterized glycoprotein containing a single *N*-linked glycosylation comprising a set of high-mannose-type glycans [14,26]. Lys-C digestion of RNaseB generated five glycopeptides, Man5–9-SRNLTK as shown in Fig. 2. Interestingly, MS spectra (Fig. 2a–c) obtained from three different positions (a, b and c) in the microscopy image gave the same pattern of signal intensities for the five glycopeptides ions. Furthermore, the MALDI images of Man5-, Man6- and Man7-SRNLTK are entirely consistent with each other, as shown in Fig. 2, indicating that they had common "sweet spots" in the MALDI sample. The detailed signal distribution obtained by scanning with a spot-to-spot center distance of 20 μm showed the same result (data not shown). This has a practical advantage because all glycoforms can be detected from common sweet spots. Hence, a reproducible glycoprofile can be obtained without scanning all the area of the sample with the laser.

3.3. Effect of glycan structures on the same peptide on signal distribution

Next, we investigated the influence of sialylation of glycopeptide on signal distribution because the character of glycopeptides occasionally differs depending upon the presence/absence of sialic acid. The preferential detachment of sialic acid residues from the glycopeptides mostly occurs in the post-source region after the ionization event. In particular, the sialic acid is easily lost in the MALDI ion trap type of mass spectrometer such as AXIMA-QIT. In the case of disialylated glycopeptides, the vast majority are detected as monosialylated species and some become completely desialylated. The signals arising from neutral glycopeptides and those from desialylated glycopeptides, which are produced *via* sialylated species, cannot be distinguished. We used a mixture of non-labeled neutral glycopeptide NA2-IRNKS and stable isotope-labeled disialylated glycopeptide A2-I*RNKS. A2-I*RNKS gave the monosialylated ion $[M\text{-NeuAc-H}]^-$ at *m*/*z* 2536.1 and small amount of the desialylated ion $[M\text{-2NeuAc-H}]^-$ at *m*/*z* 2244.9, but no intact disialylated ion. The deprotonated form of NA2-IRNKS was detected at *m*/*z* 2237.9, which could be distinguish from desialylated ion of A2-I*RNKS (Fig. 3). Although $[M-H]^-$ of A2-I*RNKS could not be detected, signal points of $[M\text{-NeuAc-H}]^-$ should be the same as those of intact molecular ion of $[M-H]^-$ because desialylation is

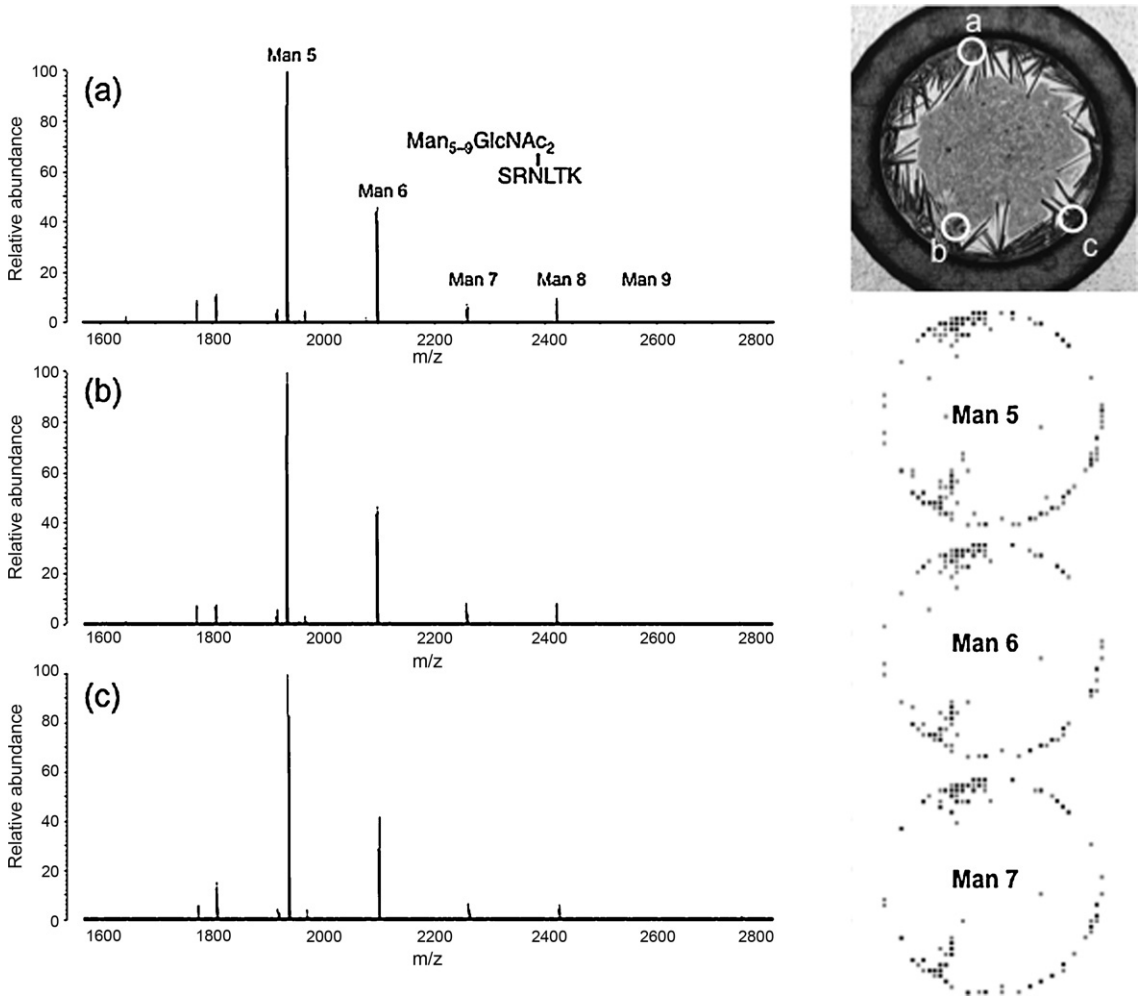

Fig. 2. Negative-ion mass spectra of glycopeptides of a Lys-C digest of RNaseB at three positions (a)–(c) as highlighted in the confocal laser microscopy image of the MALDI sample and the MS images of Man5- (*m*/*z* 1690), Man6- (*m*/*z* 1852) and Man7- (*m*/*z* 2014) glycopeptides, respectively.

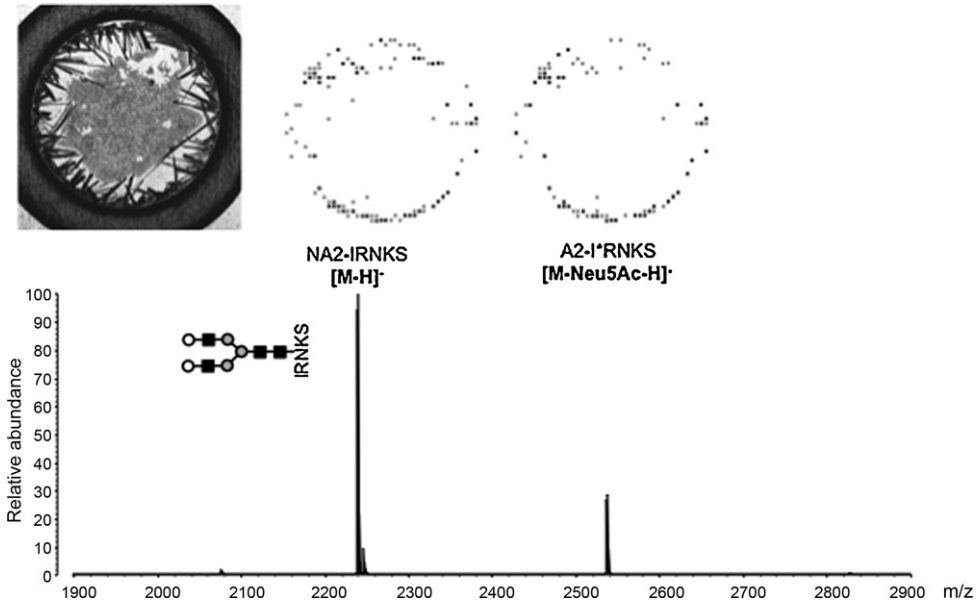

Fig. 3. The confocal laser microscopy image of the sample containing NA2-IRNKS and A2-I*RNKS, negative-ion mass spectrum and MS images. I* indicates a stable isotope-labeled isoleucine residue. The ion at *m*/*z* 2238 is used as MS image of NA2-IRNKS. The ion at *m*/*z* 2536 (A1-I*RNKS) is used as MS image of A2-I*RNKS.

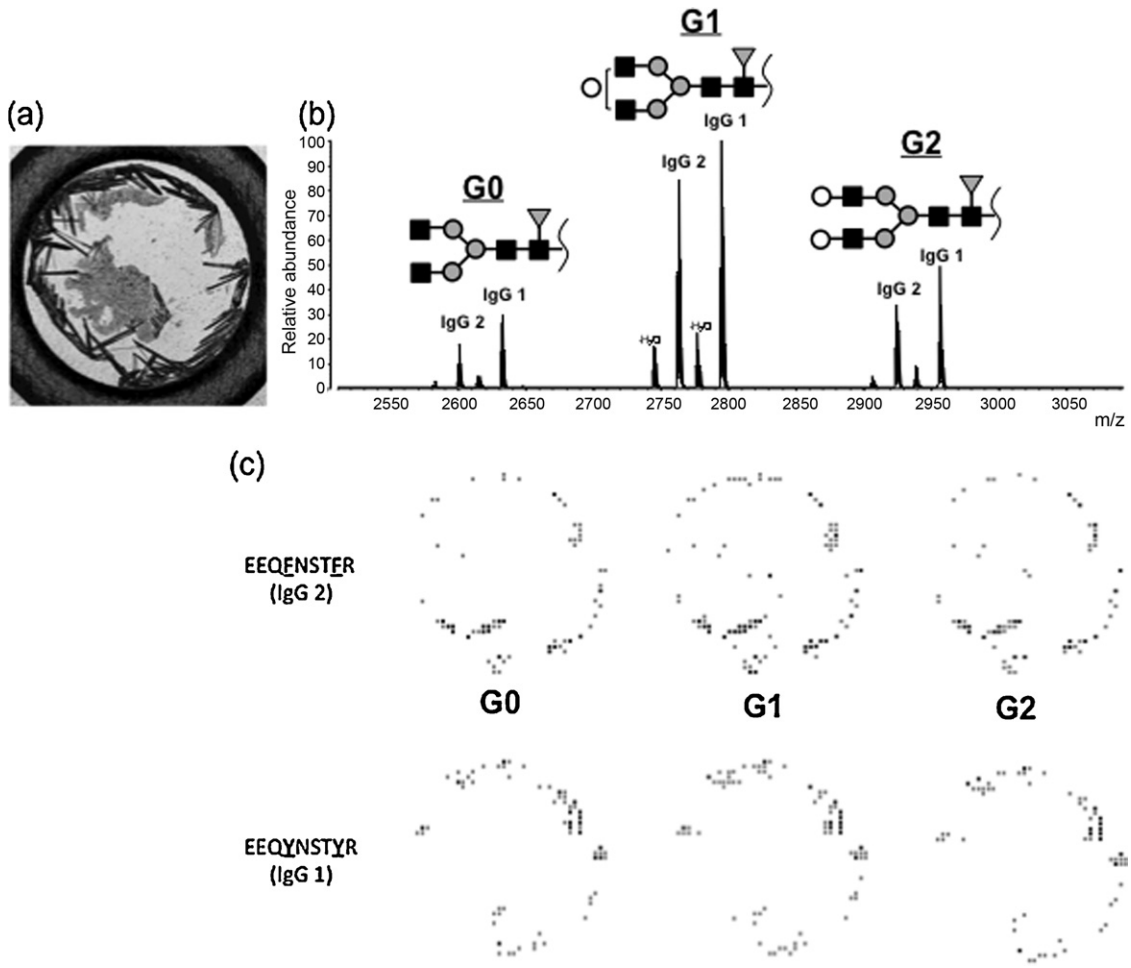

Fig. 4. The MS images of the sample containing glycopeptides derived from a tryptic digest of IgG. (a) Confocal laser microscopy image. (b) Negative-ion mass spectrum. (c) Signal distributions of G0, G1 and G2 glycopeptides derived from IgG2 and IgG1. The following ions are used as each MS image; G0-IgG1, *m*/*z* 2632; G1-IgG1, *m*/*z* 2794; G2-IgG1, *m*/*z* 2956; G0-IgG2, *m*/*z* 2600; G1-IgG2, *m*/*z* 2762; G2-IgG2, *m*/*z* 2924.

due to post-source decay. As shown in Fig. 3, positions where satisfactory signals could be obtained are very similar with NA2-IRNKS and A2-I*RNKS. These results indicate that sialylation of the glycopeptide does not affect signal distribution of the glycopeptides with the same peptide structure.

From above results signal distribution of glycopeptide is considered to be affected by peptide structure rather than glycan structure. We investigated MS images of a mixture containing NA2-IRNKS, IRNKS with the innermost GlcNAc and IRNKS without glycan. As expectedly, these three peptides showed the same signal localization (data not shown). Therefore, glycan dose not positively participate in matrix interaction. Consequently, the signals from a set of glycopeptides having the same peptide with microheterogeneity of glycan structures can be captured on the same location.

3.4. Signal distribution of a glycopeptide mixture derived from human IgG

Next, we investigated signal distribution of a mixture of glycopeptides, which have different peptides. Human IgG possesses an *N*-glycosylation site in the Fc-domain region. There are several subclasses of IgG. The amino acid sequences of tryptic peptides containing the *N*-glycosylation site are EEQYNSTYR and EEQFNSTFR for IgG1 and IgG2, respectively. *N*-Glycans on IgG are reported to be complex-type bi-antennary structures with varying numbers of galactose residues with or without core-fucosylation [27]. Six glycopeptides of IgG1 or IgG2 were detected in the preparation used in this study (Fig. 4).

As expected, G0, G1 and G2 glycopeptides derived from IgG2 gave quite similar signal distributions (Fig. 4). In the same way, the three kinds of glycopeptides derived from IgG1 also gave identical signal distributions. By contrast, however, different signal distributions were found between IgG1 glycopeptides and IgG2 glycopeptides. For example, the signal derived from G0 glycopeptide of IgG2 is not the same as that from IgG1 glycopeptide, even though the glycan structure is identical. These results again confirm that signal distribution of glycopeptide is dependent on the peptide sequences rather than glycan structures. The difference in the amino acid sequences between these glycopeptides is the substitution of two Tyr residues for Phe residues. Recently, it is reported that Tyr-296 residue in IgG1 interacts with core fucose [28]. IgG2 glycopeptides without such interaction may be different three-dimensional structure from IgG1.

Using a mixture of NA2-IRNKS and NA2-KVNKT, both MS images were the same (data not shown). These two glycopeptides are very similar and hydrophilic. These results strongly support the idea that the localization of intense signals from glycopeptides in the mixture depends on each peptide moiety.

Chymotryptic digestion of IgG results in smaller glycopeptides with the amino acid sequences of NSTY for IgG1 and NSTF for IgG2. In their mixtured sample, different MS spectra were obtained from

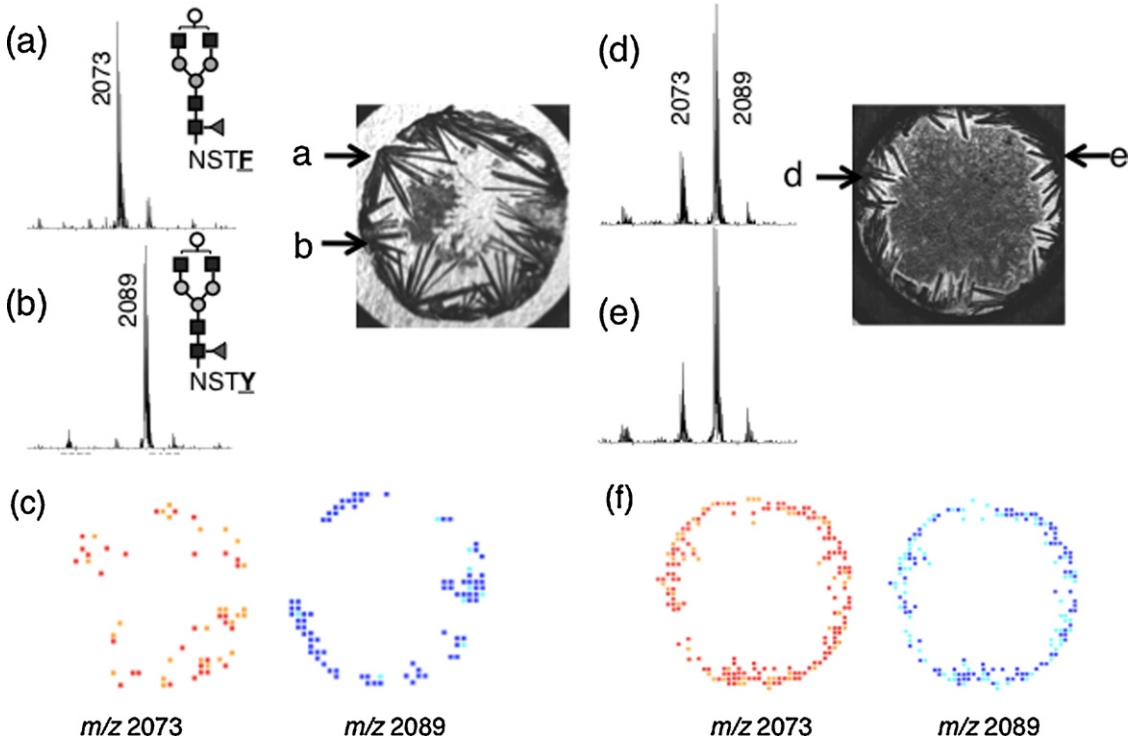

Fig. 5. The negative-ion mass spectra and MS images of the sample containing glycopeptides derived from a chymotryptic digest of IgG with (d–f) and without (a–c) pyrene derivatization. During ionization using DHBA matrix, the pyrene group is easily dissociated from glycopeptides, and almost glycopeptides can be detected as the underivatized form [12]. Therefore, the ion at *m*/*z* 2089 as G1-IgG1 and the ion at *m*/*z* 2073 as G2-IgG1 should be detected regardless derivatization.

different spots. The MS spectrum from spot a mainly shows IgG2 glycopeptide ion at *m*/*z* 2073, while only the IgG1 glycopeptide ion at *m*/*z* 2089 was found around spot b (Fig. 5a and b). MS images of these ions show quite different signal distributions, as shown in Fig. 5c. Interestingly, after pyrene derivatization of the same mixture, signals of both glycopeptides widely located at the rim and the number of spots with intense signals increased, as shown in Fig. 5f. MS spectra from different spots show the same profile (Fig. 5d and e). We already reported that pyrene derivatization of the mixture of glycopeptides and peptides selectively enhances ionization of glycopeptides but suppresses ionization of peptides [12]. These effects are found in various glycopeptides which have different amino acid sequences if the peptides are small (less than 10 amino acid residues) or hydrophilic. Pyrene derivatives have high UV photoabsorption and this nature may contribute to high ionization. In fact, laser fluence to appear ion signals for MALDI samples of pyrene-derivatized glycopeptides was less than that for MALDI samples without pyrene derivatization. In this study we discuss an advantage of pyrene derivatization from another point of view. Glycopeptides that labeled with pyrene appears to have high affinity for DHBA molecules and facilitate their incorporation into the crystals at many points, which become sweet spots. One of the reasons for high sensitivity by pyrene derivatization should be high incorporation into the matrix crystals. This effect is evenly given to glycopeptides and results in homogeneous signal distributions of them.

In fact, MALDI signal distribution is not necessarily consistent with the direct analyte distribution within the matrix crystal. The signal intensity of analyte is affected by various factors, such as purity of the sample and efficiency of ionization. In previous work, MALDI imaging techniques have been used to study the distribution of analyte in a MALDI sample [19,22,24]. Bouschen and Spengler have shown segregation of peptide analytes in small DHBA crystals in dried-droplet preparations [19]. Similar segregation of peptides within a DHBA matrix has been reported by Qiao et al. [24]. These researchers have also reported that the segregation of analytes correlates with their hydrophobicity, and to a lesser extent analyte mass or mobility. Thus, analyte co-crystallization into the matrix crystal is highly dependent on the physicochemical properties of the analyte. In this study, no segregation was observed for all glycoforms of *N*-linked glycopeptides having the same peptide moiety. These glycoforms are probably incorporated into DHBA crystals without segregating from each other. During crystallization of the sample, interaction between the growing matrix crystal and co-crystallizing glycopeptide is governed by the physicochemical properties of the peptide moiety of the glycopeptide.

We recently reported that 2,5-DHBA crystals on a target plate obtained by dried-droplet preparation contain two polymorphs and the signal inhomogeneity is highly related to both these crystal structures of 2,5-DHBA and physico-chemical properties of analyte [29]. At early stage of crystallization interaction between glycopeptides and matrix molecules makes an important role for generation of sweet spot. On this condensation process glycopeptides with the same peptide structure should act together. Furthermore, pyrene-derivatized glycopeptides have an advantage of interaction with matrix due to hydrophobicity and the result showed an increase of sweet spots regardless of crystal forms.

4. Conclusions

The current study clearly demonstrates that signal distribution of glycopeptide depends on its peptide moiety, not on the glycan structures. MALDI images of glycopeptides having the same peptide moiety are entirely consistent with each other. Hence, all glycoforms are simultaneously detected by laser irradiation to a common "sweet spot" on the MALDI sample, offering a considerable practical advantage. Data acquisition is made faster and easier by the fact that the common sweet spots result in similar spectra. Moreover, pyrene derivatization of glycopeptides enhances hydrophobicity and results in effective incorporation into the matrix crystals. As

the results, the number of sweet spots increases along the rim and MS spectra with high signal intense and homogeneity are easily obtained. Little search for better crystals is necessary, and typical shot spectra of a MALDI sample is enough without all shots over the sample, which often make low signal to noise. Thus, it should be possible to obtain accurate and reproducible MS data for microheterogeneity of glycans and site-specific glycoprofiling on the glycoprotein.

Acknowledgement

This work is supported in part by SENTAN, JST (Japan Science and Technology Agency).

References

[1] W. Morelle, K. Canis, F. Chirat, V. Faid, J.-C. Michalski, Proteomics 6 (2006) 3993.
[2] D.S. Dalpathado, H. Desaire, Analyst 133 (2008) 731.
[3] J.B. Fenn, M. Mann, C.K. Meng, S.F. Wong, C.M. Whitehouse, Science 246 (1989) 64.
[4] M. Karas, D. Bachmann, F. Hillenkamp, Analytical Chemistry 57 (1985) 2935.
[5] M. Karas, D. Bachmann, U. Bahr, F. Hillenkamp, International Journal of Mass Spectrometry and Ion Processes 87 (1987) 53.
[6] K. Tanaka, H. Waki, Y. Ido, S. Akita, Y. Yoshida, T. Yoshida, Rapid Communications in Mass Spectrometry 2 (1988) 151.
[7] M. Karas, F. Hillenkamp, Analytical Chemistry 60 (1988) 2299.
[8] D.J. Harvey, Mass Spectrometry Reviews 18 (1999) 349.
[9] D.J. Harvey, Mass Spectrometry Reviews 25 (2006) 595.
[10] D.J. Harvey, Mass Spectrometry Reviews 27 (2008) 125.
[11] J. Amano, M. Osanai, T. Orita, D. Osumi, Glycobiology 19 (2009) 601.
[12] J. Amano, T. Nishikaze, F. Tougasaki, H. Jinmei, I. Sugimoto, M. Fujita, K. Osumi, M. Mizuno, Analytical Chemistry 82 (2010) 8738.
[13] Y. Wada, P. Azadi, C.E. Costello, A. Dell, R.A. Dwek, H. Geyer, R. Geyer, K. Kakehi, N.G. Karlsson, K. Kato, N. Kawasaki, K.-H. Khoo, S. Kim, A. Kondo, E. Lattova, Y. Mechref, E. Miyoshi, K. Nakamura, H. Narimatsu, M.V. Novotny, N.H. Packer, H. Perreanlt, J. Peter-Katalinic, G. Pohlentz, V.N. Reinhold, P.M. Rudd, A. Suzuki, N. Taniguchi, Glycobiology 17 (2007) 411.
[14] M. Thaysen-Anderson, S. Mysling, P. Højrup, Analytical Chemistry 81 (2009) 3933.
[15] T. Nakamura, T. Nishikaze, H. Jinmei, F. Tougasaki, I. Sugimoto, J. Amano, Journal of Glycomics & Lipidomics 1 (2011) 103.
[16] T. Nishikaze, J. Amano, Rapid Communications in Mass Spectrometry 23 (2009) 3787.
[17] O. Vorm, P. Roepstorff, M. Mann, Analytical Chemistry 66 (1994) 3281.
[18] Y. Fukuyama, S. Nakaya, Y. Yamazaki, K. Tanaka, Analytical Chemistry 80 (2008) 2171.
[19] W. Bouschen, B. Spengler, International Journal of Mass Spectrometry 266 (2007) 129.
[20] A.I. Gusev, O.J. Vasseur, A. Proctor, A.G. Sharkey, D.M. Hercules, Analytical Chemistry 67 (1995) 4565.
[21] R.M. Caprioli, T.B. Farmer, J. Gile, Analytical Chemistry 69 (1997) 4751.
[22] R.W. Garden, J.V. Sweedler, Analytical Chemistry 72 (2000) 30.
[23] S.L. Luxembourg, L.A. McDonnel, M.C. Duursma, X. Guo, R.M.A. Heeren, Analytical Chemistry 75 (2003) 2333.
[24] H. Qiao, G. Piyadasa, V. Spicer, W. Ens, International Journal of Mass Spectrometry 281 (2009) 41.
[25] Y. Wada, M. Tajiri, S. Yoshida, Analytical Chemistry 76 (2004) 6560.
[26] H.J. An, T.R. Peavy, J.L. Hedrick, C.B. Lebrilla, Analytical Chemistry 75 (2003) 5628.
[27] C. Huhn, M.H.J. Selman, L.R. Ruhaak, A.M. Deelder, M. Wuhrer, Proteomics 9 (2009) 882.
[28] T. Mizushima, H. Yagi, E. Takemoto, M. Shibata-Koyama, Y. Isoda, S. Iida, K. Masuda, M. Satoh, K. Kato, Genes to Cells 16 (2011) 1071.
[29] T. Nishikaze, H. Okumura, H. Jinmei, J. Amano, Mass Spectrometry 1 (2012) A0006.